

RESEARCH

Open Access



Diagnosis of coronary artery disease in patients with type 2 diabetes mellitus based on computed tomography and pericoronary adipose tissue radiomics: a retrospective cross-sectional study

Xiaolin Dong^{1†}, Na Li^{1†}, Chentao Zhu¹, Yujia Wang², Ke Shi¹, Hong Pan¹, Shuting Wang¹, Zhenzhou Shi¹, Yayuan Geng³, Wei Wang^{4*} and Tong Zhang^{1*}

Abstract

Background Patients with type 2 diabetes mellitus (T2DM) are highly susceptible to cardiovascular disease, and coronary artery disease (CAD) is their leading cause of death. We aimed to assess whether computed tomography (CT) based imaging parameters and radiomic features of pericoronary adipose tissue (PCAT) can improve the diagnostic efficacy of whether patients with T2DM have developed CAD.

Methods We retrospectively recruited 229 patients with T2DM but no CAD history (146 were diagnosed with CAD at this visit and 83 were not). We collected clinical information and extracted imaging manifestations from CT images and 93 radiomic features of PCAT from all patients. All patients were randomly divided into training and test groups at a ratio of 7:3. Four models were constructed, encapsulating clinical factors (Model 1), clinical factors and imaging indices (Model 2), clinical factors and Radscore (Model 3), and all together (Model 4), to identify patients with CAD. Receiver operating characteristic curves and decision curve analysis were plotted to evaluate the model performance and pairwise model comparisons were performed via the DeLong test to demonstrate the additive value of different factors.

Results In the test set, the areas under the curve (AUCs) of Model 2 and Model 4 were 0.930 and 0.929, respectively, with higher recognition effectiveness compared to the other two models (each $p < 0.001$). Of these models, Model 2 had higher diagnostic efficacy for CAD than Model 1 ($p < 0.001$, 95% CI [0.129–0.350]). However, Model 4 did not improve the effectiveness of the identification of CAD compared to Model 2 ($p = 0.776$); similarly, the AUC did not significantly differ between Model 3 (AUC = 0.693) and Model 1 (AUC = 0.691, $p = 0.382$). Overall, Model 2 was rated better for the diagnosis of CAD in patients with T2DM.

[†]Xiaolin Dong and Na Li have contributed equally to this work

*Correspondence:

Wei Wang

1391082196@qq.com

Tong Zhang

yingxiang939@163.com

Full list of author information is available at the end of the article



Conclusions A comprehensive diagnostic model combining patient clinical risk factors with CT-based imaging parameters has superior efficacy in diagnosing the occurrence of CAD in patients with T2DM.

Keywords Type 2 diabetes mellitus, Coronary artery disease, Computed tomography

Background

Diabetes is a metabolic disorder with a high prevalence worldwide [1], with type 2 diabetes mellitus (T2DM) being the most common and highly prevalent subtype [2, 3]. Despite advances in the diagnosis and treatment of T2DM, the risk of cardiovascular disease in patients with T2DM remains high [4, 5]. Furthermore, studies have shown that coronary artery disease (CAD) is the leading cause of death in patients with T2DM [6, 7], and that CAD progresses asymptotically, only occasionally following a severe clinical course [8–10]. These findings suggest that the prevention of CAD in patients with T2DM is becoming an important public health concern. Therefore, we also need to develop new models to improve the early diagnosis of CAD in patients with T2DM to actively prevent the development and progression of CAD.

Coronary computed tomography angiography (CTA) is considered an important modality for the noninvasive diagnosis of CAD in patients with T2DM [11, 12]; therefore, some of the imaging parameters obtained by coronary CTA are increasingly becoming auxiliary indicators for the diagnosis and stratification of CAD. Computed tomography (CT)-based fractional flow reserve (CT-FFR), with invasive FFR as the gold standard, has been shown to be highly accurate in the diagnosis of CAD as an indicator of functional myocardial ischaemia [13–15]. Furthermore, coronary artery calcium is an important marker for identifying CAD [16], and a high coronary artery calcium score (CACS) has been found to be a predictor of CAD and is independently associated with the occurrence of cardiovascular events [17, 18]. Vascular inflammation is a major driver of atherosclerosis and plaque rupture [19], and pericoronary adipose tissue (PCAT) based on coronary CTA has been demonstrated in recent years as a new sensitive marker to indicate the degree of coronary inflammation, which can be used to identify and stratify CAD [20]. The CRISP-CT study found that significantly higher PCAT attenuation (PCATA) around the left anterior descending artery (LAD) and right coronary artery (RCA) was an important risk factor for increased cardiac mortality [21]. PCATA has consequently been recognized as an important marker of increased cardiovascular risk. The onset of inflammation alters the composition of PCAT via various processes, such as fibrosis and microvascular remodeling [22, 23], and radiomics analysis captures these subtle structural remodelling processes to reflect permanent

changes in adipose tissue [24]. Radiomics extracts multiple features embedded in medical images to establish machine learning models [24].

In recent years, an increasing number of studies have examined patients with T2DM, and a higher LAD-PCATA [25], plaque volume and mild calcification [26], and increased epicardial adipose tissue volume [27] have been found to improve the prediction of future cardiovascular events and cardiogenic death in patients with T2DM. A higher CACS has also been shown to be an independent predictor of CAD in patients with T2DM [28]. However, these studies have focused on future cardiac death and serious cardiovascular events, such as heart failure, and no studies have yet combined the data for the early identification of patients with T2DM and CAD. Therefore, we aimed to explore the risk factors associated with patients with T2DM and CAD and to identify patients with suspected CAD in T2DM by establishing a model combining clinical data, CT-based imaging parameters and PCAT-radiomics. The resultant data were used to establish an appropriate diagnostic model to monitor patients with T2DM, reduce the coronary burden and save their lives at an early stage.

Methods

Study population

We retrospectively recruited patients with diabetes who were continuously admitted to the Department of Endocrinology at the Fourth Affiliated Hospital of Harbin Medical University from June 2020 to May 2022, including patients with previously diagnosed diabetes and those diagnosed during the current visit. A total of 337 patients underwent noncontrast chest CT and coronary CTA scans during this hospitalization for typical or atypical chest pain, and all had fasting blood samples taken for laboratory analysis within 24 h of admission. We excluded patients with previous coronary revascularisation (n=28); previous cardiac diseases, including CAD (n=45), myocardial infarction (n=1) and pericarditis (n=2); a history of tumours or active tumours (n=5); type 1 diabetes mellitus (n=1); contrast allergy (n=4); poor image quality (n=14); incomplete clinical information (n=2); and coronary CTA with CT interval >7 days (n=6). Ultimately, 229 T2DM patients were included in this study, of whom 146 patients were diagnosed with CAD by invasive coronary angiography at this visit, including 109 patients with stable CAD and 37 patients

with acute coronary syndrome; the remaining 83 patients did not develop CAD. Figure 1 illustrates the selection and exclusion of patients.

Data collection

Two radiologists jointly collected the baseline features of the patients from clinical inpatient records, such as age, sex, body mass index (BMI), laboratory test data, previous medication use, CAD risk factors and diabetes-related complications. CAD, known as coronary atherosclerotic heart disease, is defined as heart disease caused by atherosclerosis of the coronary arteries that results in the narrowing or blockage of the lumen, leading to ischaemia, hypoxia or necrosis of the myocardium. CAD is divided into two main categories: stable CAD and acute coronary syndrome. Risk factors for CAD are classified according to the following criteria: (A) Hypertension: systolic blood pressure >140 mmHg and/or diastolic blood pressure >90 mmHg and/or use of antihypertensive medication according to the guidelines [29]; (B) Dyslipidaemia: dyslipidaemia defined as fasting total cholesterol >6.2 mmol/L, low-density lipoprotein (LDL) cholesterol >3.4 mmol/L, high-density lipoprotein (HDL) cholesterol <1.0 mmol/L, serum triglycerides >1.7 mmol/L (outpatient only), or diagnosis/treatment of dyslipidaemia [30]; (C) Diabetes mellitus: patients on oral hypoglycaemic agents or insulin or with

fasting blood glucose ≥ 7.0 mmol/L are defined as T2DM [31]; (D) Family history of CAD: family history of ≥ 1 degree of consanguinity with CAD before age 60 [20]; (E) Obesity: BMI ≥ 28 kg/m² is considered to be obese [32]. Diabetes-related complications include (A) retinopathy: any medical basis for retinopathy; (B) neuropathy: any sign or symptom of polyneuropathy; (C) peripheral arterial occlusive disease: 50% stenosis on ultrasonography; and (D) nephropathy: renal failure, i.e., glomerular filtration rate <60 mL/min and/or micro or macro proteinuria [33, 34].

CT image acquisition

All scans were performed on a 320-detector-row CT scanner (Aquilion ONE, Toshiba, Tokyo, Japan). The patients underwent a noncontrast chest CT on admission from the thoracic inlet to the abdomen. The patients also underwent coronary CTA scans during their hospital stay. All patients with a rapid heart rate at baseline were given an oral beta-blocker (25–75 mg) 1 h before the examination to reduce the heart rate to ≤ 65 beats/min. A dual-channel high-pressure syringe was used to inject 60–80 mL of nonionic iodine contrast agent (iohexol injection containing 350 mg/L iodine, GE Healthcare, Beijing, China) at a flow rate of 4.5 mL/s, and coronary CTA image acquisition was performed using prospective ECG-triggered. The acquisition and reconstruction

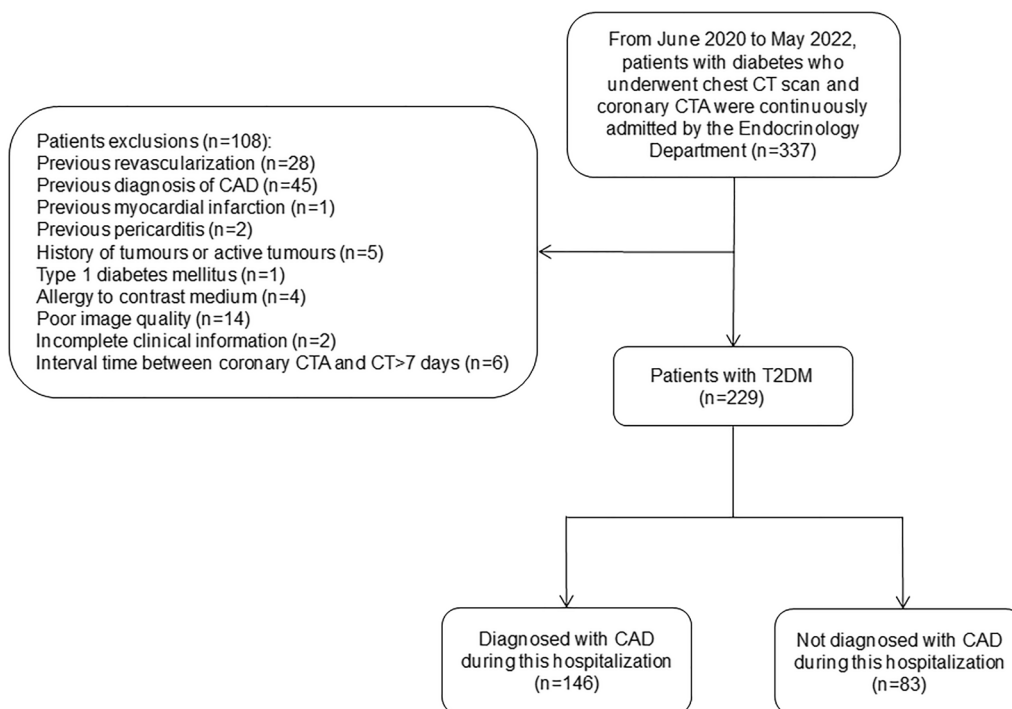


Fig. 1 Flowchart showing inclusion and exclusion criteria for the study population. CT computed tomography, CTA computed tomography angiography, CAD coronary artery disease, T2DM type 2 diabetes mellitus

parameters in our study were as follows: 275 ms/time rack rotation speed, 120 kV tube potential, automatic adjustment of tube current according to patient BMI, 0.5 mm slice increments, images with 512×512 matrix and 0.25 mm or 0.5 mm increments. All scans were carried out during a single breath-hold. Two experienced cardiovascular imaging investigators interpreted the acquired imaging findings.

Acquisition of image parameters and radiomic features

Based on noncontrast CT images [35], the CACS was calculated using the uAI Sphere (United Imaging Intelligence, v1.0.8214.7256) via the Agatston method [36], which is based on the principle of calcification density fractionation \times calcification area (mm^2). Plaques with CT values of 130–199, 200–299, 300–399 and ≥ 400 Hounsfield units (HU) were assigned a density score corresponding to 1, 2, 3 or 4, respectively. The scores for individual coronary arteries in all sections were summed to obtain the total coronary calcification score. The pericardial adipose tissue (PAT) volume was quantified using syngo.via (Siemens Healthcare GmbH, v06.07.0000.0000), which automatically calculates the total volume of tissue in the pericardial CT density range from -190 HU to -30 HU [37]. Using the semiautomatic quantification software CoronaryDoc[®]-FFR (Shukun (Beijing) Network Technology, v1.11.1), CT-FFR was calculated by combining the reduced-order method [38] and machine-learning modification [39]. Diameter stenosis (DS) was also quantified using the same software and was defined as (reference diameter–minimum lumen diameter)/reference diameter, patients with stenosis $>50\%$ were considered to have significant stenosis [40]. PCAT was measured quantitatively using CoronaryDoc[®]. PCAT was defined as adipose tissue located within a radial distance from the outer vessel wall equal to the diameter of the coronary artery and with a CT attenuation range of -190 HU to -30 HU [21]. We tracked adipose tissue around three coronary trunks using an automated method, the 40 mm length range proximal to the LAD and left circumflex artery (LCX) and the 10 mm to 50 mm length segment proximal to the RCA. Figure 2 demonstrates an example of the abovementioned parameters. Moreover, we extracted 93 radiomic features from each PCAT (Additional file 1) from CoronaryDoc[®]. All imaging parameters were measured jointly by two radiologists, with a senior radiologist involved in case of disagreement.

Model building and clinical application

This study divided the dataset into training and test cohorts at a ratio of 7:3 at random. To select the most representative radiomic features, least absolute shrinkage and selection operator (LASSO) was applied, and

the best lambda was determined with tenfold cross validation. Radscore [41] was added to other models to represent imaging features (detailed formula is listed in Additional file 1). Significant clinical factors and imaging indices were identified by univariate logistic regression with $p < 0.05$. Generalized logistic models were consecutively established with only clinical factors (Model 1), clinical factors and imaging indices (Model 2), clinical factors and Radscore (Model 3), and all together (Model 4) to examine their effect on discriminating patients with CAD from those without CAD. Sensitivity, specificity, accuracy, negative predictive value (NPV), positive predictive value (PPV) and area under the curve (AUC) were calculated to evaluate model performance. The DeLong test was performed to compare performance between models in a pairwise manner, and decisive curve analysis (DCA) was also plotted to assess clinical validity. The nomogram of the best model was illustrated according to the generalized logistic model. Figure 3 shows the workflow diagram for this study.

Statistical analysis

The normality of continuous data was tested using the Shapiro–Wilk test. Continuous variables are expressed as the mean \pm standard deviation of normally distributed variables and median interquartile range of nonnormally distributed variables. Comparisons were made using Student's t test or the Mann–Whitney U test, as needed. Categorical variables are then expressed as absolute frequencies and percentages and were compared using the χ^2 test or Fisher's exact test. Independent influences on patients with T2DM combined with CAD were identified using univariate and multivariate logistic regression analyses. A receiver operating characteristic (ROC) curve was used to evaluate the diagnostic efficacy of the four models for the diagnosis of CAD in patients with T2DM. A two-tailed $p < 0.05$ was considered statistically significant. R software (v4.1.0) and MedCalc (v20.115) were used for the statistical analysis and image plotting in this study.

Results

Patient characteristics

A total of 229 patients with T2DM were included in this study. The mean age of the patients was 58.79 ± 9.32 years, with 60.7% of patients being male. The clinical and imaging parameters of T2DM patients with and without CAD are shown in Table 1. Overall, 146 patients were diagnosed with CAD for the first time at this screening. Patients diagnosed with CAD were generally older ($p < 0.001$), more likely to have hypertension ($p = 0.007$) and dyslipidaemia ($p = 0.008$), and had higher levels of fasting glucose ($p = 0.001$) and glycated haemoglobin (HbA1c) ($p < 0.001$) than

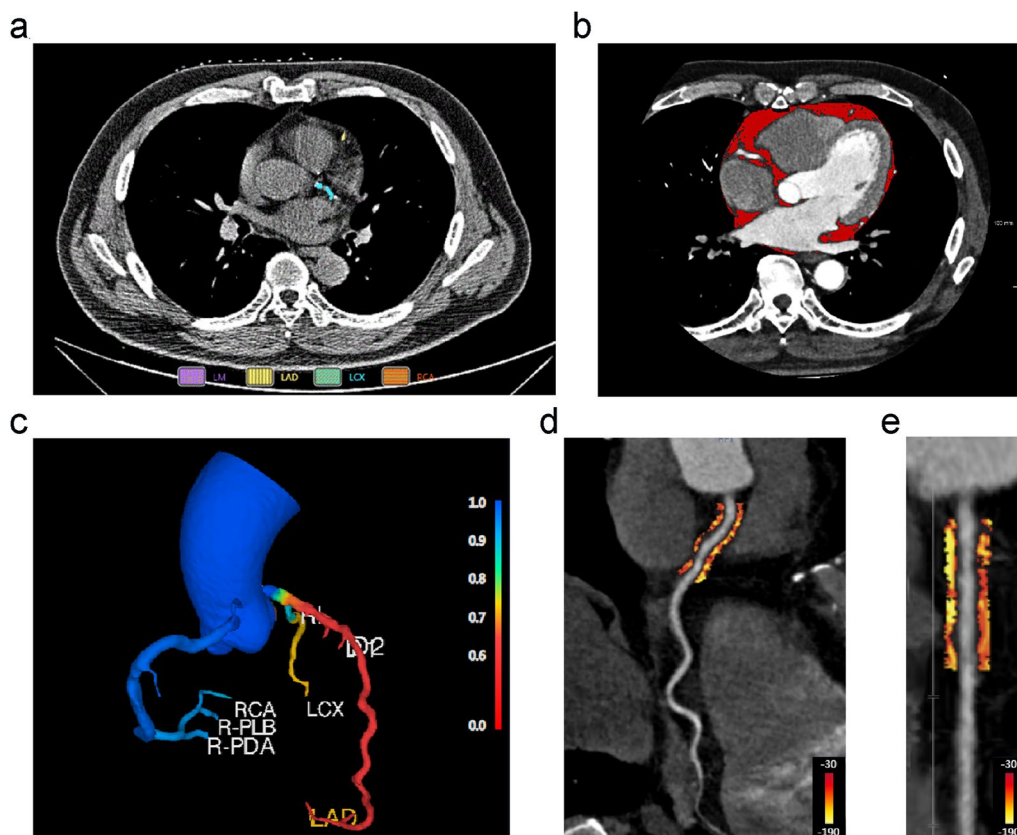


Fig. 2 Representative case of imaging parameters measured by noncontrast chest CT and coronary CTA. **a** Example diagram of CACS measurements, yellow indicates calcification on LAD and green indicates calcification on LCX; **b** PAT volume measurement, red areas indicate pericardial adipose tissue; **c** CT-FFR model, CT-FFR values are marked in blue to red in the colour bar; **d** Curved multiplanar view showing PCAT quantification around the proximal coronary artery within reference diameter from the outer wall of the vessel, PCAT is visualized with adipose tissue HU colour table shown with colour bars; **e** shows the segment of the proximal coronary artery in a straightened view. *CT* computed tomography, *CTA* computed tomography angiography, *CACS* coronary artery calcium score, *PAT* pericardial adipose tissue, *CT-FFR* computed tomography-based fractional flow reserve, *PCAT* pericoronary adipose tissue

the remaining patients in the cohort. Remarkably, the time since T2DM diagnosis was longer in patients with concomitant CAD ($p < 0.001$). The CACS, CT-FFR, DS and PCATA significantly differed between patients with concomitant CAD and those without CAD (each $p \leq 0.001$). The clinical and imaging characteristics of the patients in the training and test sets are shown in (Additional file 1: Table S1).

Model establishment

Twenty-six radiomic features were selected as important features via LASSO and individual coefficients are plotted in (Additional file 1: Fig. S1). Six clinical factors and 6 imaging indicators were selected as important risk factors in univariate logistic regression (Table 2). Furthermore, multivariate logistic regression showed that age, HbA1c, CACS, CT-FFR, DS and RCA-PCATA were independent indicators in distinguishing CAD patients (each $p < 0.05$).

Model performance and pairwise comparison

The ROC curves of the four models in the training and test sets are plotted in Fig. 4. Models 1 and 3 were quite similar in performance, and the same trend appeared for Models 2 and 4. Table 3 shows the detailed model performance parameters, such as AUC, sensitivity, specificity, accuracy, PPV and NPV, in both datasets. Models 2 and 4 achieved the most encouraging results, with AUCs of 0.960 [0.934–0.987] and 0.930 [0.871–0.989] for Model 2 and 0.961 [0.934–0.988] and 0.929 [0.869–0.989] for Model 4 in the training and test datasets, respectively; both models produced significantly different results than Models 1 and 3 (each $p < 0.001$, DeLong test, detailed results in Additional file 1: Table S2). The diagnostic value of Model 2 for CAD was markedly higher than that of Model 1, with a significant difference between the AUCs of the two models ($p < 0.001$, 95% CI [0.129–0.350]). Notable, adding the Radscore to Models 1 and 2 did not significantly improve the recognition performance of the

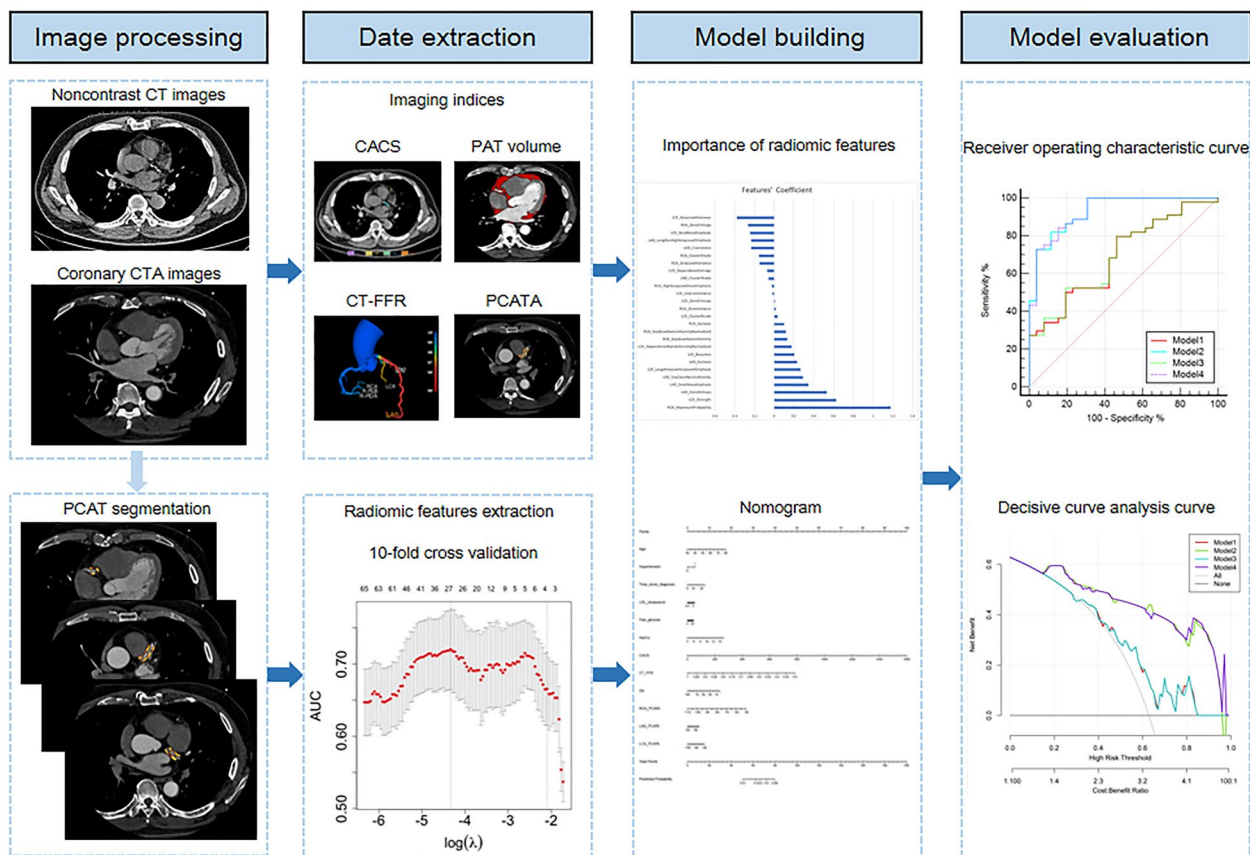


Fig. 3 A flow chart of model development. CTA computed tomography angiography, CT computed tomography, PCAT pericoronary adipose tissue, CACS coronary artery calcium score, PAT pericardial adipose tissue, CT-FFR computed tomography-based fractional flow reserve, PCATA pericoronary adipose tissue attenuation

models (each $p > 0.05$). Model 2 can be further developed as a quantitative tool for the subsequent identification of the probability of CAD occurrence in patients with T2DM, which we present in the form of a nomogram (Fig. 5). The DCA curve indicated that Models 2 and 4 could add more benefit than Models 1 and 3 (Fig. 6).

Effect of the degree of stenosis

We grouped all patients with T2DM according to whether significant stenosis occurred in the coronary arteries. Patients with T2DM with significant stenosis had higher CACS ($p < 0.001$), lower CT-FFR ($p < 0.001$) and higher PCATA around the three coronary arteries ($p < 0.05$), but the PAT volume did not significantly differ between the two groups ($p = 0.325$) (Additional file 1: Table S3). The same results were obtained for patients with T2DM without significant stenosis (Additional file 1: Table S4). However, when patients with T2DM with CAD were divided into two groups based on the presence or absence of significant stenosis, the RCA-PCATA significantly differed between groups ($p = 0.020$),

whereas the LAD-PCATA and LCX-PCATA did not significantly differ between groups (each $p > 0.05$) (Additional file 1: Table S5). Compared with patients without CAD, patients with T2DM with CAD demonstrated more serious disease progression, as evidenced by the CACS, CT-FFR and RCA-PCATA, irrespective of the presence of significant stenosis, but patients with significant stenosis had a heavier coronary burden than those without significant stenosis.

Discussion

In this study, four models were developed to diagnose CAD in patients with T2DM, and their performance was validated in all aspects. Both the model combining clinical risk characteristics and CT imaging parameters as well as the combined model were found to be superior in identifying the occurrence of CAD, but Model 4, which added the Radscore to Model 2, did not improve the diagnostic performance compared to Model 2. We also developed a nomogram to diagnose patients with T2DM with CAD for future clinical applications. Additionally,

Table 1 Comparison of characteristics between T2DM patients with and without CAD

Characteristic	All	Patient with CAD	Patient without CAD	p
n	229	146	83	
Age (years)	58.79 ± 9.32	60.36 ± 9.01	56.02 ± 9.27	< 0.001
Male sex, n (%)	139 (60.7)	92 (63.0)	47 (56.6)	0.341
Body mass index (kg/m ²)	26.00 [23.68; 27.70]	26.00 [23.60; 27.40]	25.70 [23.80; 28.10]	0.608
Obesity, n (%)	50 (21.8)	28 (19.2)	22 (26.5)	0.197
Smoking, n (%)	51 (22.3)	35 (24.0)	16 (19.3)	0.412
Drinking, n (%)	28 (12.2)	21 (14.4)	7 (8.4)	0.186
Hypertension, n (%)	142 (62.0)	100 (68.5)	42 (50.6)	0.007
Dyslipidaemia, n (%)	25 (10.9)	22 (15.1)	3 (3.6)	0.008
Family history, n (%)	20 (8.7)	15 (10.3)	5 (6.0)	0.274
Time since T2DM diagnosis (years)	7.00 [2.00; 12.25]	10.00 [4.00; 15.00]	3.00 [0.00; 8.00]	< 0.001
Aspirin, n (%)	12 (5.2)	9 (6.2)	3 (3.6)	0.405
Statin, n (%)	93 (40.6)	60 (41.1)	33 (39.8)	0.843
Metformin, n (%)	108 (47.2)	69 (47.3)	39 (47.0)	0.968
Insulin, n (%)	96 (41.9)	59 (40.4)	37 (44.6)	0.539
Oral antihyperglycemic drugs, n (%)	195 (85.2)	126 (86.3)	69 (83.1)	0.517
HDL-cholesterol (mg/dL)	0.99 [0.87; 1.12]	0.98 [0.86; 1.10]	1.02 [0.91; 1.17]	0.102
LDL-cholesterol (mg/dL)	3.43 [3.01; 3.79]	3.58 [3.09; 3.97]	3.28 [2.77; 3.53]	< 0.001
Total cholesterol (mg/dL)	5.28 [3.91; 6.00]	5.44 [3.99; 6.17]	4.66 [3.78; 5.78]	0.031
Triglyceride (mg/dL)	1.86 [0.65; 2.80]	0.83 [0.52; 2.72]	2.09 [0.93; 2.87]	0.003
Fast glucose (mmol/L)	9.60 [7.90; 12.21]	10.20 [8.30; 12.70]	8.80 [7.23; 11.28]	0.001
HbA1c (%)	7.70 [6.80; 9.10]	8.10 [7.40; 9.30]	7.00 [6.33; 8.43]	< 0.001
Retinopathy, n (%)	132 (57.6)	86 (58.9)	46 (55.4)	0.608
Neuropathy, n (%)	215 (93.9)	137 (93.8)	78 (94.0)	0.966
Peripheral arterial occlusive disease, n (%)	175 (76.4)	113 (77.4)	62 (74.7)	0.644
Nephropathy, n (%)	83 (36.2)	54 (37.0)	29 (34.9)	0.757
CACS	28.69 [4.15; 127.07]	70.68 [15.66; 224.41]	7.48 [1.61; 24.60]	< 0.001
PAT volume (mL)	178.44 [135.41; 230.29]	180.14 [138.64; 243.55]	173.55 [131.60; 212.33]	0.289
CT-FFR	0.83 [0.71; 0.90]	0.75 [0.64; 0.85]	0.90 [0.86; 0.94]	< 0.001
DS (%)	48.00 [22.00; 67.00]	57.50 [34.00; 72.00]	28.00 [0.00; 52.00]	< 0.001
RCA-PCATA (HU)	− 84.13 ± 9.64	− 80.94 ± 8.84	− 89.75 ± 8.38	< 0.001
LAD-PCATA (HU)	− 82.90 ± 8.59	− 80.50 [− 87.00; − 74.00]	− 86.00 [− 91.00; − 81.00]	< 0.001
LCX-PCATA (HU)	− 80.00 [− 87.00; − 74.00]	− 78.68 ± 8.06	− 84.00 ± 7.38	< 0.001

Values are mean ± standard deviation, median [25th and 75th percentile] or n (%). p values signify statistical significance and reflect the differences between patients with and without CAD. Obesity was defined as a body mass index ≥ 28 kg/m²

T2DM type 2 diabetes mellitus, CAD coronary artery disease, HDL high-density lipoprotein, LDL low-density lipoprotein, HbA1c glycated haemoglobin, CACS coronary artery calcium score, PAT pericardial adipose tissue, CT-FFR computed tomography-based fractional flow reserve, DS diameter stenosis, PCATA pericoronary adipose tissue attenuation

patients with T2DM with CAD have a higher coronary burden, regardless of whether significant coronary stenosis has occurred.

Patients with T2DM have higher levels of chronic inflammation in the coronary vasculature because the high glycaemic state of the blood promotes the infiltration of macrophages and T cells [40, 42], causing aggregation of foam cells [43], while vascular inflammation leads to increased concentrations of circulating cytokines thus leading to atherosclerosis [44]. Therefore, T2DM is

considered an independent risk factor for atherosclerosis that increases the risk of cardiovascular disease [26]. The T2DM population is considered to be a heterogeneous group of patients with and without CAD [28], and CAD is gaining attention as a major cause of death in T2DM. Therefore, we plan to develop a model to identify patients with T2DM and concomitant CAD. Previous studies have shown that the CACS can be used as a proxy for coronary atherosclerotic plaque burden to predict cardiovascular risk [45], and the CACS increases

Table 2 Logistics regression analysis of factors associated with CAD

Characteristics	Univariable			Multivariable		
	OR	95%CI	p	OR	95%CI	p
Age	1.054	1.017–1.092	0.004	1.117	1.029–1.213	0.009
Gender	1.454	0.755–2.801	0.263			
BMI	0.990	0.904–1.084	0.832			
Obesity	0.664	0.313–1.408	0.286			
Smoking	1.350	0.623–2.927	0.447			
Drinking	1.935	0.669–5.594	0.223			
Hypertension	2.013	1.027–3.946	0.042	2.974	0.748–11.821	0.122
Dyslipidaemia	3.349	0.932–12.035	0.064			
Family history	3.667	0.791–17.003	0.097			
Time since T2DM diagnosis	1.145	1.076–1.219	<0.001	1.086	0.973–1.212	0.138
Aspirin	1.719	0.335–8.81	0.516			
Statin	1.106	0.566–2.159	0.768			
Metformin	1.231	0.642–2.361	0.532			
Insulin	0.641	0.333–1.234	0.184			
Oral antihyperglycemic drugs	2.023	0.865–4.730	0.104			
HDL-cholesterol	0.327	0.083–1.290	0.110			
LDL-cholesterol	1.523	1.014–2.288	0.043	1.208	0.508–2.872	0.670
Total cholesterol	1.236	0.985–1.551	0.067			
Triglyceride	1.006	0.856–1.183	0.941			
Fast glucose	1.202	1.067–1.354	0.003	1.037	0.825–1.305	0.753
HbA1c	1.505	1.197–1.894	<0.001	1.597	1.048–2.434	0.029
Retinopathy	1.407	0.734–2.697	0.303			
Neuropathy	1.208	0.326–4.470	0.778			
Peripheral arterial occlusive disease	1.821	0.843–3.933	0.127			
Nephropathy	0.976	0.498–1.912	0.943			
CACS	1.021	1.010–1.031	<0.001	1.020	1.006–1.034	0.003
PAT volume	1.004	1.000–1.008	0.055			
CT-FFR	0.000	0.000–0.000	<0.001	0.000	0.000–0.000	<0.001
DS	1.038	1.024–1.052	<0.001	0.954	0.918–0.993	0.018
RCA-PCATA	1.100	1.052–1.149	<0.001	1.151	1.052–1.260	0.002
LAD-PCATA	1.042	1.003–1.083	0.036	0.964	0.88–1.054	0.424
LCX-PCATA	1.078	1.031–1.127	0.001	1.063	0.956–1.181	0.260

CAD coronary artery disease, OR odds ratio, 95%CI 95% confidence interval, T2DM type 2 diabetes mellitus, HDL high-density lipoprotein, LDL low-density lipoprotein, HbA1c glycated haemoglobin, CACS coronary artery calcium score, PAT pericardial adipose tissue, CT-FFR computed tomography-based fractional flow reserve, DS diameter stenosis, PCATA pericoronary adipose tissue attenuation

with cardiovascular risk in the T2DM patient population [46] to serve as a composite measure of atherosclerotic disease [16]. CT-FFR, as an indicator of coronary vascular haemodynamic stenosis, provides both physiological and corresponding anatomical information about the coronary vessels [47]; DS directly reflects the anatomical stenosis of the coronary vessels. Whereas PAT is located near the myocardium, and its excessive activity accelerates coronary atherosclerosis and, thus, cardiovascular disease [48]. However, logistic regression analysis revealed that PAT volume was not an influential factor in the development of CAD in patients with T2DM, and

we speculate that this lack of influence may be because PAT is not in direct contact with the myocardium; therefore, PAT is not directly influenced by paracrine signals from the myocardium [23], which is similar to the findings of a previous study [27]. As adipose tissue is closer to the coronary arteries, there is a closer bidirectional influence between PCAT and the coronary vessel wall [49]; inflammatory changes in the coronary arteries affect alterations in the water–lipid balance in PCAT [49], causing dynamic changes in PCATA and similarly in high-dimensional features, and the discovery of such alterations in fine structure relies on the application of

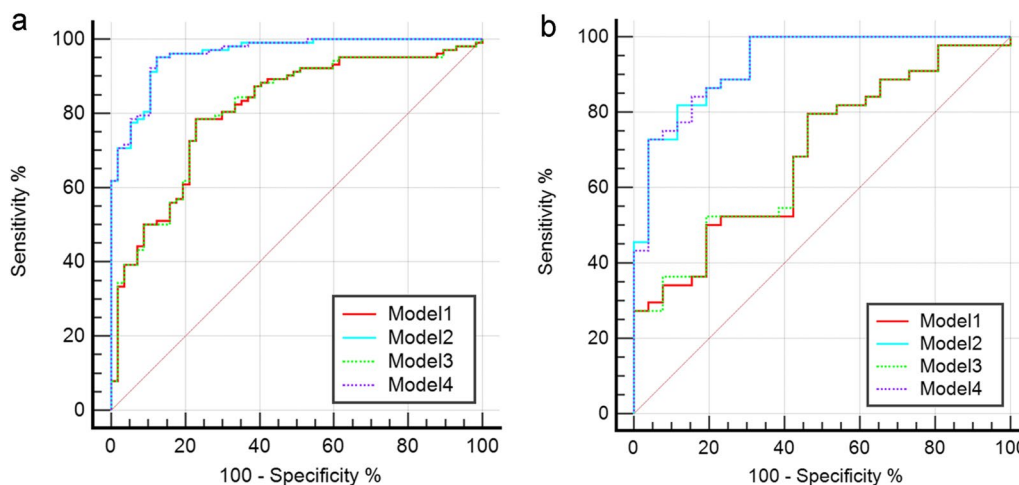


Fig. 4 Receiver operating characteristic curves of all models in the training **a** and test **b** sets. *Model 1* clinical factors model, *Model 2* clinical factors and imaging indexes model, *Model 3* clinical factors and Radscore model, *Model 4* combined model

Table 3 Recognition ability of all models for patients with CAD

Model	Training set						Test set					
	AUC (95%CI)	SEN	SPE	ACC	PPV	NPV	AUC (95%CI)	SEN	SPE	ACC	PPV	NPV
Model 1	0.811(0.741–0.881)	0.784	0.772	0.780	0.667	0.860	0.691(0.564–0.817)	0.577	0.659	0.629	0.500	0.725
Model 2	0.960(0.934–0.987)	0.951	0.877	0.925	0.909	0.933	0.930(0.871–0.989)	0.885	0.773	0.814	0.697	0.919
Model 3	0.812(0.742–0.882)	0.784	0.772	0.780	0.667	0.860	0.693(0.567–0.819)	0.577	0.659	0.629	0.500	0.725
Model 4	0.961(0.934–0.988)	0.951	0.877	0.925	0.909	0.933	0.929(0.869–0.989)	0.885	0.773	0.814	0.697	0.919

AUC area under curve, 95%CI 95% confidence interval, SEN sensitivity, SPE specificity, ACC accuracy, PPV positive predictive value, NPV negative predictive value

Model 1 clinical factors model

Model 2 clinical factors and imaging indexes model

Model 3 clinical factors and Radscore model

Model 4 combined model

radiomics [24, 50]. In particular, age and HbA1c levels were independently associated with the development of CAD among the patients’ clinical risk factors by multivariate logistic regression analysis. We assume that this result may be because older patients have more severe cardiovascular ageing and consequently have a more severe cardiovascular risk [51]. Moreover, HbA1c indicates the patient’s glycaemic control, and poor glycaemic control (HbA1c ≥ 7.0%) can lead to endothelial dysfunction, which negatively impacts the coronary arteries [52].

Our study used logistic regression to screen for clinical factors and CT imaging indices associated with the development of CAD and additionally combined the radiomic parameters of PCAT to develop a model to identify patients with T2DM and concomitant CAD. This study is the first to combine multiple factors to diagnose the occurrence of CAD in patients with T2DM. While previous studies have focused on the future occurrence of late cardiovascular events in patients with T2DM [25–27, 45], we have focused on CAD with the aim of detecting

the onset of CAD before an irreversible endpoint event occurs in patients with T2DM. We have developed an optimal model nomogram to help patients proactively monitor the progression of their disease and the probability of CAD based on their condition and examination findings to proactively prevent and treat CAD in a timely manner. Alternatively, previous studies have reported that anti-inflammatory interventions and statin therapy result in a significant reduction in PCATA [53, 54], which may affect the subsequent clinical performance of patients with T2DM. Thus, we also collected patients’ medication history, including not only aspirin and statins but also various types of hypoglycaemic drugs. Regrettably, these drugs were not found to be associated with the development of CAD when the initial parametric screening was performed.

Our study combined a variety of CT imaging indices based on clinical factors. First, the Agatston-based CACS was included in the model, and previous studies have also identified the CACS as a risk factor for the

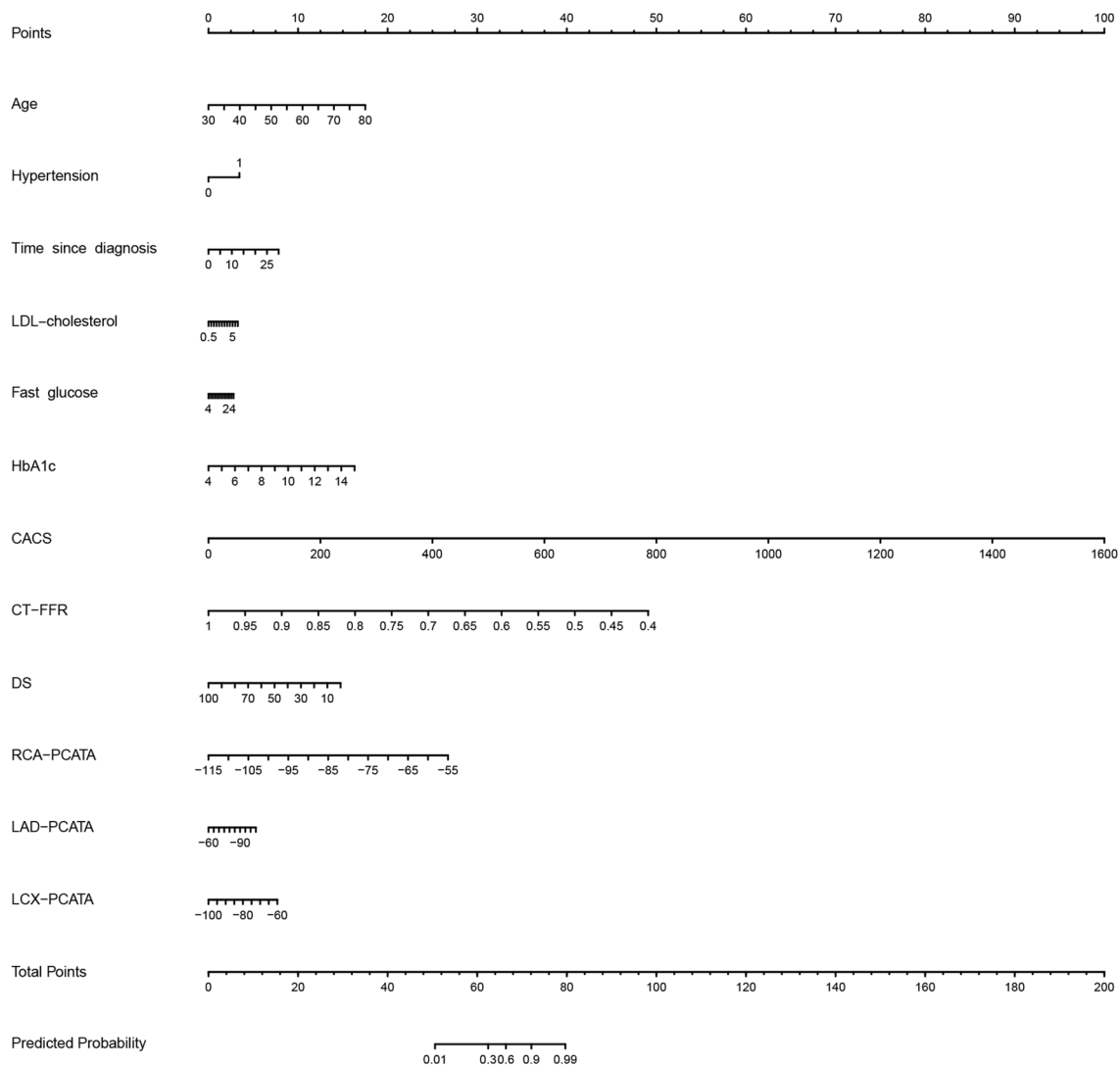


Fig. 5 The nomogram of Model 2. The sum of all factors equals the total points. *Model 2* clinical factors and imaging indexes model, *LDL* low-density lipoprotein, *HbA1c* glycated haemoglobin, *CACS* coronary artery calcium score, *CT-FFR* computed tomography-based fractional flow reserve, *DS* diameter stenosis, *PCATA* pericoronary adipose tissue attenuation

development of CAD in patients with T2DM [28], mainly because the CACS, which is based on direct measurements of the Agatston score, represents the extent and severity of atherosclerosis [55], which provides a direct response to coronary artery calcification. Whereas CT-FFR and DS reflect functional stenosis and anatomical stenosis of the coronary arteries, respectively, CT-FFR has also been shown in the past to provide greater accuracy in predicting coronary haemodynamic lesions [39]. In contrast, PCATA has been more extensively studied, and the value of a higher PCATA in predicting future cardiovascular events in patients with T2DM has been demonstrated [25]. Conversely, we found that RCA-PCATA was more heavily represented than LAD and LCX in

the model for identifying CAD and that it was an independent influence on CAD occurrence, possibly because compared to the other two coronary trunks, there is less interference near the RCA, the measurements are more accurate, and the correlation with coronary inflammation has been validated at the molecular biological level [49]. Yu et al. also suggest that RCA-PCATA can be used to capture early inflammation around the coronary arteries [40]. Unexpectedly, however, the addition of radiomics to either Model 1 or 2 did not improve the model's identification efficacy. We suspected that the reason for this lack of improvement is that in patients with T2DM, the coronary arteries have already undergone a certain degree of inflammatory changes, which affect the

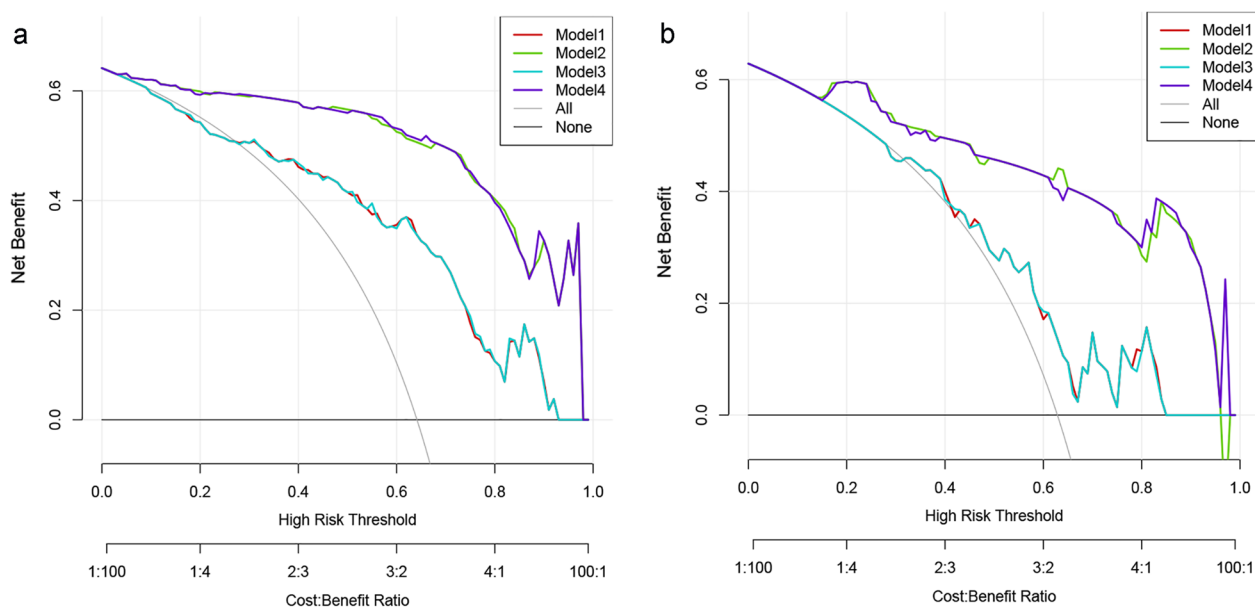


Fig. 6 Decision curve analysis for the four models in the training **a** and test **b** sets. *Model 1* clinical factors model, *Model 2* clinical factors and imaging indexes model, *Model 3* clinical factors and Radscore model, *Model 4* combined model

spatial distribution of voxel intensity of PCAT in CTA images [56]. Furthermore, the effect on the spatial position of voxels in the images may be weakened when CAD occurs on this basis. Second, CT parameters that reflect functional and anatomical changes in the coronary arteries may be more valuable for the diagnosis of CAD in patients with T2DM than radiomics. Furthermore, we found that more than half of the patients were diagnosed with CAD, which we believe may be because diabetes is an independent risk factor for cardiovascular disease, and indeed, patients with T2DM have a very high probability of cardiovascular events; moreover, coronary CTA is not a routine test, and some of the patients with T2DM who participated in this test had symptoms or signs related to CAD detected during hospitalization, either clinically or by electrocardiogram, and thus using coronary CTA to supplement diagnosis.

We have developed a more comprehensive model for diagnosing CAD in patients with T2DM that incorporates the patient's clinical risk factors and CT imaging parameters. The nomogram created by this model captures the probability of CAD risk in patients with T2DM and allows for a noninvasive method of discerning the existence of CAD in patients. Thus, this model allows for a more proactive approach to prevent development and progression of CAD. As a noninvasive rapid diagnostic aid, the model can help clinicians and patients with T2DM to monitor and identify CAD early and in real time during the subclinical period before it progresses to have clinical manifestations. Clinicians can then

aggressively deploy treatment to reduce the cardiovascular burden and risk of death for patients due to CAD. Treatment may even be implemented before the development of CAD, promoting the evolution of precision medicine. The measurements of the imaging parameters in this study were fully automated, which greatly improves the reproducibility of the study. Our patient cohort was smaller than those in previous studies [57, 58], but we collected more comprehensive clinical information than previous studies, measured a more comprehensive range of CT imaging parameters, and combined these data with radiomic parameters that have emerged in recent years to obtain a more efficient model.

This study was subject to several limitations that need to be addressed. First, this work was a single-centre retrospective study, and all patients used the same CT scan protocol with some selection bias. Therefore, more external validation is needed to improve the generalizability of the model. Second, our study demonstrates that the occurrence of T2DM with CAD is independently correlated with some clinical and CT imaging parameters but does not suggest a direct causal relationship between these parameters. Third, our study is a cross-sectional observational study, and we currently cannot describe the changes in the PCATA, CT-FFR and CACS over the course of the patients' disease. The next step is to collect relevant data for follow-up observation. Fourth, we can only know the type of medication used by the patients in the past but not the duration of medication use. Finally, some patients were restricted from receiving coronary

CTA due to severe renal insufficiency, and this group of patients is consequently not represented in our study. In the future, we will consider conducting relevant studies mainly in patients with renal insufficiency.

Conclusions

Our study shows that a model based on clinical features and CT imaging indices has the highest efficacy in diagnosing the occurrence of CAD in patients with T2DM. Our findings may help clinicians and patients with T2DM monitor and rapidly identify CAD in real time, provide timely diagnosis and treatment, and reduce future deaths due to cardiovascular disease.

Abbreviations

T2DM	Type 2 diabetes mellitus
CAD	Coronary artery disease
CTA	Computed tomography angiography
CT	Computed tomography
CT-FFR	Computed tomography-based fractional flow reserve
CACS	Coronary artery calcium score
PCAT	Pericoronary adipose tissue
PCATA	Pericoronary adipose tissue attenuation
LAD	Left anterior descending artery
RCA	Right coronary artery
BMI	Body mass index
LDL	Low-density lipoprotein
HDL	High-density lipoprotein
HU	Hounsfield units
PAT	Pericardial adipose tissue
DS	Diameter stenosis
LCX	Left circumflex artery
LASSO	Least absolute shrinkage and selection operator
AUC	Area under the curve
NPV	Negative predictive value
PPV	Positive predictive value
DCA	Decisive curve analysis
ROC	Receiver operating characteristic
HbA1c	Glycated haemoglobin

Supplementary Information

The online version contains supplementary material available at <https://doi.org/10.1186/s12933-023-01748-0>.

Additional file 1. Table S1. Baseline characteristics of the training set and test set. **Table S2.** Pairwise comparison of the AUCs of the test set by the DeLong test. **Table S3.** Comparison of CT parameters in patients with T2DM with significant coronary stenosis. **Table S4.** Comparison of CT parameters in patients with T2DM without significant coronary stenosis. **Table S5.** Comparison of CT parameters in patients with CAD with and without significant stenosis. **Figure S1.** The relative importance of radiomics features.

Acknowledgements

We thank Lin Li from the Department of Radiology, The Fourth Affiliated Hospital of Harbin Medical University, China, for her guidance and assistance in the interpretation of cardiovascular imaging results.

Author contributions

XD and NL contributed to the conception and design, acquisition, analysis and interpretation of the work and drafted the manuscript. CZ, YW, KS, HP, SW and ZS contributed to data acquisition. YG contributed to data analysis

and revised the manuscript. TZ and WW revised the manuscript. All gave final approval and agreed to be accountable for all aspects of the work, ensuring integrity and accuracy. All authors read and approved the final manuscript.

Funding

This work was supported by the Beijing Cihua Medical Development Foundation Project (Research on CT-assisted diagnosis of coronary heart disease based on artificial intelligence).

Availability of data and materials

The datasets used and/or analysed during the current study are available from the corresponding author on reasonable request.

Declarations

Ethics approval and consent to participate

The study protocol was approved by the Medical Ethics Committee of The Fourth Affiliated Hospital of Harbin Medical University (No. 2022-WZYS-LLSC-34) and conducted in accordance with the principles contained within the Declaration of Helsinki, but patient informed consent was waived because it was a retrospective study.

Consent for publication

Not applicable.

Competing interests

YG is employed by Shukun (Beijing) Network Technology, and the authors declare that they have no competing interests.

Author details

¹Department of Radiology, Fourth Affiliated Hospital of Harbin Medical University, No. 37, YiYuan Street, NanGang District, Harbin 150001, Heilongjiang, China. ²Department of Interventional and Vascular, Fourth Affiliated Hospital of Harbin Medical University, No. 37, YiYuan Street, NanGang District, Harbin 150001, Heilongjiang, China. ³Shukun (Beijing) Network Technology Co., Ltd, Jinhui Building, Qiyang Road, Beijing 100102, China. ⁴The MRI Room, First Affiliated Hospital of Harbin Medical University, No. 23, YouZheng Street, NanGang District, Harbin 150001, Heilongjiang, China.

Received: 8 December 2022 Accepted: 18 January 2023

Published online: 23 January 2023

References

1. Group IDFDA. Update of mortality attributable to diabetes for the IDF diabetes atlas: estimates for the year 2013. *Diabetes Res Clin Pract.* 2013;109(3):461–5.
2. Cavender MA, Steg PG, Smith SC Jr, Eagle K, Ohman EM, Goto S, Kuder J, Im K, Wilson PW, Bhatt DL. Impact of diabetes mellitus on hospitalization for heart failure, cardiovascular events, and death: outcomes at 4 years from the reduction of Atherothrombosis for continued health (REACH) registry. *Circulation.* 2015;132(10):923–31.
3. Saeedi P, Petersohn I, Salpea P, Malanda B, Karuranga S, Unwin N, Colagiuri S, Guariguata L, Motala AA, Ogurtsova K, et al. Global and regional diabetes prevalence estimates for 2019 and projections for 2030 and 2045: Results from the International Diabetes Federation Diabetes Atlas, 9(th) edition. *Diabetes Res Clin Pract.* 2019;157:107843.
4. Gregg EW, Li Y, Wang J, Burrows NR, Ali MK, Rolka D, Williams DE, Geiss L. Changes in diabetes-related complications in the United States, 1990–2010. *N Engl J Med.* 2014;370(16):1514–23.
5. Vergès B. Cardiovascular disease in type 1 diabetes: a review of epidemiological data and underlying mechanisms. *Diabetes Metab.* 2020;46(6):442–9.
6. Arnett DK, Blumenthal RS, Albert MA, Buroker AB, Goldberger ZD, Hahn EJ, Himmelfarb CD, Khera A, Lloyd-Jones D, McEvoy JW, et al. 2019 ACC/AHA guideline on the primary prevention of cardiovascular disease: executive summary: a report of the American college of cardiology/american heart association task force on clinical practice guidelines. *Circulation.* 2019;140(11):e563–95.

7. Schramm TK, Gislason GH, Køber L, Rasmussen S, Rasmussen JN, Abildstrøm SZ, Hansen ML, Folke F, Buch P, Madsen M, et al. Diabetes patients requiring glucose-lowering therapy and nondiabetics with a prior myocardial infarction carry the same cardiovascular risk: a population study of 3.3 million people. *Circulation*. 2008;117(15):1945–54.
8. Jouven X, Lemaître RN, Rea TD, Sotoodehnia N, Empana JP, Siscovick DS. Diabetes, glucose level, and risk of sudden cardiac death. *Eur Heart J*. 2005;26(20):2142–7.
9. Sarwar N, Gao P, Seshasai SR, Gobin R, Kaptoge S, Di Angelantonio E, Ingelsson E, Lawlor DA, Selvin E, Stampfer M, et al. Diabetes mellitus, fasting blood glucose concentration, and risk of vascular disease: a collaborative meta-analysis of 102 prospective studies. *Lancet*. 2010;375(9733):2215–22.
10. Whiteley L, Padmanabhan S, Hole D, Isles C. Should diabetes be considered a coronary heart disease risk equivalent?: results from 25 years of follow-up in the Renfrew and Paisley survey. *Diabetes Care*. 2005;28(7):1588–93.
11. Narula J, Chandrasekhar Y, Ahmadi A, Abbara S, Berman DS, Blankstein R, Leipsic J, Newby D, Nicol ED, Nieman K, et al. SCCT 2021 expert consensus document on coronary computed tomographic angiography: a report of the society of cardiovascular computed tomography. *J Cardiovasc Comput Tomogr*. 2021;15(3):192–217.
12. Scholte AJ, Schuijff JD, Kharagjitsingh AV, Jukema JW, Pundziute G, van der Wall EE, Bax JJ. Prevalence of coronary artery disease and plaque morphology assessed by multi-slice computed tomography coronary angiography and calcium scoring in asymptomatic patients with type 2 diabetes. *Heart*. 2008;94(3):290–5.
13. Coenen A, Kim YH, Kruk M, Tesche C, De Geer J, Kurata A, Lubbers ML, Daemen J, Itu L, Rapaka S, et al. Diagnostic accuracy of a machine-learning approach to coronary computed tomographic angiography-based fractional flow reserve: result from the machine consortium. *Circ Cardiovasc Imaging*. 2018;11(6):e007217.
14. Tesche C, De Cecco CN, Baumann S, Renker M, McLaurin TW, Duguay TM, Bayer RR 2nd, Steinberg DH, Grant KL, Canstein C, et al. Coronary CT angiography-derived fractional flow reserve: machine learning algorithm versus computational fluid dynamics modeling. *Radiology*. 2018;288(1):64–72.
15. Zhang JM, Han H, Tan RS, Chai P, Fam JM, Teo L, Chin CY, Ong CC, Low R, Chandola G, et al. diagnostic performance of fractional flow reserve from CT coronary angiography with analytical method. *Front Cardiovasc Med*. 2021;8:739633.
16. Greenland P, Blaha MJ, Budoff MJ, Erbel R, Watson KE. Coronary calcium score and cardiovascular risk. *J Am Coll Cardiol*. 2018;72(4):434–47.
17. Budoff MJ, Young R, Burke G, Jeffrey Carr J, Detrano RC, Folsom AR, Kronmal R, Lima JAC, Liu KJ, McClelland RL, et al. Ten-year association of coronary artery calcium with atherosclerotic cardiovascular disease (ASCVD) events: the multi-ethnic study of atherosclerosis (MESA). *Eur Heart J*. 2018;39(25):2401–8.
18. Li Y, Liu B, Li Y, Jing X, Deng S, Yan Y, She Q. Epicardial fat tissue in patients with diabetes mellitus: a systematic review and meta-analysis. *Cardiovasc Diabetol*. 2019;18(1):3.
19. Si N, Shi K, Li N, Dong X, Zhu C, Guo Y, Hu J, Cui J, Yang F, Zhang T. Identification of patients with acute myocardial infarction based on coronary CT angiography: the value of pericoronary adipose tissue radiomics. *Eur Radiol*. 2022. <https://doi.org/10.1007/s00330-022-08812-5>.
20. Lin A, Nerlekar N, Yuvaraj J, Fernandes K, Jiang C, Nicholls SJ, Dey D, Wong DTL. Pericoronary adipose tissue computed tomography attenuation distinguishes different stages of coronary artery disease: a cross-sectional study. *Eur Heart J Cardiovasc Imaging*. 2021;22(3):298–306.
21. Oikonomou EK, Marwan M, Desai MY, Mancio J, Alashi A, Hutt Centeno E, Thomas S, Herdman L, Kotanidis CP, Thomas KE, et al. Non-invasive detection of coronary inflammation using computed tomography and prediction of residual cardiovascular risk (the CRISP CT study): a post-hoc analysis of prospective outcome data. *Lancet*. 2018;392(10151):929–39.
22. Crewe C, An YA, Scherer PE. The ominous triad of adipose tissue dysfunction: inflammation, fibrosis, and impaired angiogenesis. *J Clin Invest*. 2017;127(1):74–82.
23. Oikonomou EK, Antoniades C. The role of adipose tissue in cardiovascular health and disease. *Nat Rev Cardiol*. 2019;16(2):83–99.
24. Oikonomou EK, Williams MC, Kotanidis CP, Desai MY, Marwan M, Antonopoulos AS, Thomas KE, Thomas S, Akoumianakis I, Fan LM, et al. A novel machine learning-derived radiotranscriptomic signature of perivascular fat improves cardiac risk prediction using coronary CT angiography. *Eur Heart J*. 2019;40(43):3529–43.
25. Ichikawa K, Miyoshi T, Osawa K, Nakashima M, Miki T, Nishihara T, Toda H, Yoshida M, Ito H. High pericoronary adipose tissue attenuation on computed tomography angiography predicts cardiovascular events in patients with type 2 diabetes mellitus: post-hoc analysis from a prospective cohort study. *Cardiovasc Diabetol*. 2022;21(1):44.
26. Halon DA, Lavi I, Barnett-Griness O, Rubinshtein R, Zafrir B, Azencot M, Lewis BS. Plaque morphology as predictor of late plaque events in patients with asymptomatic type 2 diabetes: a long-term observational study. *JACC Cardiovasc Imaging*. 2019;12(7 Pt 2):1353–63.
27. Christensen RH, von Scholten BJ, Hansen CS, Jensen MT, Vilsbøll T, Rossing P, Jørgensen PG. Epicardial adipose tissue predicts incident cardiovascular disease and mortality in patients with type 2 diabetes. *Cardiovasc Diabetol*. 2019;18(1):114.
28. Takamura K, Fujimoto S, Mita T, Kawaguchi YO, Kurita M, Kadowaki S, Kamo Y, Aoshima C, Nozaki YO, Takahashi D, et al. Identification of risk factors for coronary artery disease in asymptomatic patients with type 2 diabetes mellitus. *J Clin Med*. 2022. <https://doi.org/10.3390/jcm11051226>.
29. Williams B, Mancia G, Spiering W, Agabiti Rosei E, Azizi M, Burnier M, Clement DL, Coca A, de Simone G, Dominiczak A, et al. 2018 ESC/ESH Guidelines for the management of arterial hypertension. *Eur Heart J*. 2018;39(33):3021–104.
30. Jacobson TA, Ito MK, Maki KC, Orringer CE, Bays HE, Jones PH, McKenney JM, Grundy SM, Gill EA, Wild RA, et al. National lipid association recommendations for patient-centered management of dyslipidemia: part 1—full report. *J Clin Lipidol*. 2015;9(2):129–69.
31. Classification and Diagnosis of Diabetes. Standards of medical care in diabetes—2020. *Diabetes Care*. 2020;43(Suppl 1):S14–s31.
32. Chinese Medical Association EB. Medicine DBotCSotC, committee of obesity and diabetes surgeons CPA, branch of surgeons, hospitals DaOSCotCSor: multidisciplinary clinical consensus on diagnosis and treatment of obesity (2021 edition). *Chinese J Endocrinol Metabolism*. 2021;37(11):959–72.
33. Cosson E, Nguyen MT, Rezgani I, Berkane N, Pinto S, Bihan H, Tatulashvili S, Taher M, Sal M, Soussan M, et al. Epicardial adipose tissue volume and myocardial ischemia in asymptomatic people living with diabetes: a cross-sectional study. *Cardiovasc Diabetol*. 2021;20(1):224.
34. Cosson E, Nguyen MT, Rezgani I, Tatulashvili S, Sal M, Berkane N, Allard L, Brillat PY, Bihan H. Epicardial adipose tissue volume and coronary calcification among people living with diabetes: a cross-sectional study. *Cardiovasc Diabetol*. 2021;20(1):35.
35. Huili S, Jie C, Huan Z, Bin C, Chao G, Xiaoyin W, Ning G, Zhiqun W. Accuracy evaluation of coronary artery calcification score by non gated chest CT scan based on artificial intelligence technology. *Computerized Tomography Theory and Applications*. 2021;30(1):106–13.
36. Agatston AS, Janowitz WR, Hildner FJ, Zusmer NR, Viamonte M Jr, Detrano R. Quantification of coronary artery calcium using ultrafast computed tomography. *J Am Coll Cardiol*. 1990;15(4):827–32.
37. Shah RV, Anderson A, Ding J, Budoff M, Rider O, Petersen SE, Jensen MK, Koch M, Allison M, Kawel-Boehm N, et al. Pericardial, but not hepatic, fat by CT is associated with CV outcomes and structure: the multi-ethnic study of Atherosclerosis. *JACC Cardiovasc Imaging*. 2017;10(9):1016–27.
38. Müller LO, Fossan FE, Bråten AT, Jørgensen A, Wiseth R, Hellevik LR. Impact of baseline coronary flow and its distribution on fractional flow reserve prediction. *Int J Numer Method Biomed Eng*. 2021;37(11):e3246.
39. Yu M, Lu Z, Shen C, Yan J, Wang Y, Lu B, Zhang J. The best predictor of ischemic coronary stenosis: subtended myocardial volume, machine learning-based FFR(CT), or high-risk plaque features? *Eur Radiol*. 2019;29(7):3647–57.
40. Yu Y, Ding X, Yu L, Dai X, Wang Y, Zhang J. Increased coronary pericoronary adipose tissue attenuation in diabetic patients compared to non-diabetic controls: a propensity score matching analysis. *J Cardiovasc Comput Tomogr*. 2022;16(4):327–35.
41. Huang Y, Liu Z, He L, Chen X, Pan D, Ma Z, Liang C, Tian J, Liang C. Radiomics signature: a potential biomarker for the prediction of disease-free survival in early-stage (I or II) non-small cell lung cancer. *Radiology*. 2016;281(3):947–57.
42. Calle MC, Fernandez ML. Inflammation and type 2 diabetes. *Diabetes Metab*. 2012;38(3):183–91.

43. Kaplan M, Kerry R, Aviram M, Hayek T. High glucose concentration increases macrophage cholesterol biosynthesis in diabetes through activation of the sterol regulatory element binding protein 1 (SREBP1): inhibitory effect of insulin. *J Cardiovasc Pharmacol*. 2008;52(4):324–32.
44. Puglisi MJ, Fernandez ML. Modulation of C-reactive protein, tumor necrosis factor-alpha, and adiponectin by diet, exercise, and weight loss. *J Nutr*. 2008;138(12):2293–6.
45. Ichikawa K, Miyoshi T, Osawa K, Miki T, Toda H, Ejiri K, Yoshida M, Nanba Y, Yoshida M, Nakamura K, et al. Prognostic value of non-alcoholic fatty liver disease for predicting cardiovascular events in patients with diabetes mellitus with suspected coronary artery disease: a prospective cohort study. *Cardiovasc Diabetol*. 2021;20(1):8.
46. Cosentino F, Grant PJ, Aboyans V, Bailey CJ, Ceriello A, Delgado V, Federici M, Filippatos G, Grobbee DE, Hansen TB, et al. 2019 ESC Guidelines on diabetes, pre-diabetes, and cardiovascular diseases developed in collaboration with the EASD. *Eur Heart J*. 2020;41(2):255–323.
47. Shi K, Yang FF, Si N, Zhu CT, Li N, Dong XL, Guo Y, Zhang T. Effect of 320-row CT reconstruction technology on fractional flow reserve derived from coronary CT angiography based on machine learning: single-versus multiple-cardiac periodic images. *Quant Imaging Med Surg*. 2022;12(6):3092–103.
48. Packer M. Critical role of the epicardium in mediating cardiac inflammation and fibrosis in patients with type 2 diabetes. *Diabetes Obes Metab*. 2019;21(8):1765–8.
49. Antonopoulos AS, Sanna F, Sabharwal N, Thomas S, Oikonomou EK, Herdman L, Margaritis M, Shirodaria C, Kampoli AM, Akoumianakis I, et al. Detecting human coronary inflammation by imaging perivascular fat. *Sci Transl Med*. 2017. <https://doi.org/10.1126/scitranslmed.aal2658>.
50. Cheng K, Lin A, Yuvaraj J, Nicholls SJ, Wong DTL. Cardiac computed tomography radiomics for the non-invasive assessment of coronary inflammation. *Cells*. 2021. <https://doi.org/10.3390/cells10040879>.
51. Masoli JAH, Mensah E, Rajkumar C. Age and ageing cardiovascular collection: blood pressure, coronary heart disease and heart failure. *Age Ageing*. 2022. <https://doi.org/10.1093/ageing/afac179>.
52. Chen S, Shen Y, Liu YH, Dai Y, Wu ZM, Wang XQ, Yang CD, Li LY, Liu JM, Zhang LP, et al. Impact of glycemic control on the association of endothelial dysfunction and coronary artery disease in patients with type 2 diabetes mellitus. *Cardiovasc Diabetol*. 2021;20(1):64.
53. Elnabawi YA, Oikonomou EK, Dey AK, Mancio J, Rodante JA, Aksentjevich M, Choi H, Keel A, Erb-Alvarez J, Teague HL, et al. Association of Biologic Therapy With Coronary Inflammation in Patients With Psoriasis as Assessed by Perivascular Fat Attenuation Index. *JAMA Cardiol*. 2019;4(9):885–91.
54. Dai X, Yu L, Lu Z, Shen C, Tao X, Zhang J. Serial change of perivascular fat attenuation index after statin treatment: Insights from a coronary CT angiography follow-up study. *Int J Cardiol*. 2020;319:144–9.
55. Baumgart D, Schmermund A, Goerge G, Haude M, Ge J, Adamzik M, Sehnert C, Altmaier K, Groenemeyer D, Seibel R, et al. Comparison of electron beam computed tomography with intracoronary ultrasound and coronary angiography for detection of coronary atherosclerosis. *J Am Coll Cardiol*. 1997;30(1):57–64.
56. Kolossváry M, Kellermayer M, Merkely B, Maurovich-Horvat P. Cardiac Computed Tomography Radiomics: A Comprehensive Review on Radiomic Techniques. *J Thorac Imaging*. 2018;33(1):26–34.
57. Choi Y, Yang Y, Hwang BH, Lee EY, Yoon KH, Chang K, Jaffer FA, Cho JH. Practical cardiovascular risk calculator for asymptomatic patients with type 2 diabetes mellitus: PRECISE-DM risk score. *Clin Cardiol*. 2020;43(9):1040–7.
58. Shimabukuro M, Saito T, Higa T, Nakamura K, Masuzaki H, Sata M. Risk stratification of coronary artery disease in asymptomatic diabetic subjects using multidetector computed tomography. *Circ J*. 2015;79(11):2422–9.

Publisher's Note

Springer Nature remains neutral with regard to jurisdictional claims in published maps and institutional affiliations.

Ready to submit your research? Choose BMC and benefit from:

- fast, convenient online submission
- thorough peer review by experienced researchers in your field
- rapid publication on acceptance
- support for research data, including large and complex data types
- gold Open Access which fosters wider collaboration and increased citations
- maximum visibility for your research: over 100M website views per year

At BMC, research is always in progress.

Learn more biomedcentral.com/submissions

